microLife, 2022, **3**, 1–12
DOI: 10.1093/femsml/uqac015
Advance access publication date: 21 September 2022
Research Article

Cryptococcus neoformans releases proteins during intracellular residence that affect the outcome of the fungal–macrophage interaction

Eric H. Jung[1], Yoon-Dong Park[2], Quigly Dragotakes[1], Lia S. Ramirez[3], Daniel Q. Smith[1], Flavia C. G. Reis[4,6], Amanda Dziedzic[1], Marcio L. Rodrigues[4,7], Rosanna P. Baker[1], Peter R. Williamson[2], Anne Jedlicka[1], Arturo Casadevall[1,*,†], Carolina Coelho[5,*,†]

[1]Department of Molecular Microbiology and Immunology, Johns Hopkins School of Public Health, 615 North Wolfe Street, Baltimore, MD 21205, United States
[2]Laboratory of Clinical Immunology and Microbiology, National Institute of Allergy and Infectious Disease, National Institutes of Health, Memorial Drive, Bethesda, MD 20814, United States
[3]Department of Molecular and Cell Biology, Johns Hopkins University, 615 North Wolfe Street, Baltimore, MD 21205, United States
[4]Instituto Carlos Chagas, Fundação Oswaldo Cruz (Fiocruz), Rua Professor Algacyr Munhoz Mader, 3775, Curitiba - PR, 81310-020, Brazil
[5]MRC Centre for Medical Mycology, College of Health and Medicine, University of Exeter, Stocker Road, Exeter EX4 4QD, Devon, United Kingdom
[6]Centro de Desenvolvimento Tecnológico em Saúde (CDTS), Fundação Oswaldo Cruz Av. Brasil 4036. Room 814, Rio de Janeiro - RJ, 21040-361, Brazil
[7]Instituto de Microbiologia Paulo de Góes (IMPG), Universidade Federal do Rio de Janeiro, Rio de Janeiro Cidade Universitária da Universidade Federal do Rio de Janeiro,, Rio de Janeiro - RJ, 21941-902, Brazil
*__Corresponding author:__ Department of Molecular Microbiology and Immunology, Johns Hopkins School of Public Health, 615 N, Wolfe Street, Room E5132, Baltimore, MD 21205, United States. E-mail: acasade1@jhu.edu. Medical Research Council Centre for Medical Mycology at University of Exeter, College of Health and Medicine, Geoffrey Pope Building, Room 325, University of Exeter, Stocker Road, Exeter EX4 4QD, Devon, United Kingdom. **E-mail:**c.coelho@exeter.ac.uk
†CC and AC share senior authorship.
Editor: Carmen Buchrieser

Abstract

Cryptococcus neoformans is a facultative intracellular pathogen that can replicate and disseminate in mammalian macrophages. In this study, we analyzed fungal proteins identified in murine macrophage-like cells after infection with *C. neoformans*. To accomplish this, we developed a protocol to identify proteins released from cryptococcal cells inside macrophage-like cells; we identified 127 proteins of fungal origin in infected macrophage-like cells. Among the proteins identified was urease, a known virulence factor, and others such as transaldolase and phospholipase D, which have catalytic activities that could contribute to virulence. This method provides a straightforward methodology to study host–pathogen interactions. We chose to study further Yeast Oligomycin Resistance (Yor1), a relatively uncharacterized protein belonging to the large family of ATP binding cassette transporter (ABC transporters). These transporters belong to a large and ancient protein family found in all extant phyla. While ABC transporters have an enormous diversity of functions across varied species, in pathogenic fungi they are better studied as drug efflux pumps. Analysis of *C. neoformans yor1*Δ strains revealed defects in nonlytic exocytosis, capsule size, and dimensions of extracellular vesicles, when compared to wild-type strains. We detected no difference in growth rates and cell body size. Our results indicate that *C. neoformans* releases a large suite of proteins during macrophage infection, some of which can modulate fungal virulence and are likely to affect the fungal–macrophage interaction.

Keywords: *Cryptococcus neoformans*, fungal, extracellular vesicles, Yor1, secreted, proteins/virulence factors, Yor1 (Yeast Oligomycin Resistance 1)

Introduction

Cryptococcus neoformans is a basidiomycetous opportunistic fungal pathogen found worldwide (Casadevall and Perfect 1998). Human infection occurs when desiccated yeasts or spores are inhaled into the lung, where the infection is controlled in the majority of immunologically intact individuals (May et al. 2016). However, in many immunocompromised individuals, such as patients with HIV/AIDS or those on an immunosuppressive therapy, the infection is no longer controlled and cryptococcosis ensues, which often manifests itself as a subacute meningoencephalitis, i.e. inevitably fatal if not treated with antifungal agents. While this disease predominantly affects immunocompromised individuals, it occurs sporadically in immunocompetent individuals (Fisher et al. 2016). Cryptococcosis results in approximately 180 000 deaths per annum, primarily in sub Saharan Africa, where HIV/AIDS prevalence is high (Rajasingham et al. 2017).

Cryptococcus neoformans is a facultative intracellular pathogen that can replicate inside macrophages (Feldmesser et al. 2000) and the topic has been the subject of several recent reviews (Coelho et al. 2014, Gilbert et al. 2014, Mansour et al. 2014, DeLeon-Rodriguez and Casadevall 2016). There is a correlation between the susceptibility of mice and rats to cryptococcosis and the ability of *C. neoformans* to replicate within macrophages (Shao et al. 2005, Zaragoza et al. 2007). In both mice and zebrafish, increases in *C. neoformans* numbers are associated with the ability of fungal cells to replicate in macrophages (Feldmesser et al. 2000, Bojarczuk et al. 2016). In humans, there is a correlation between disease outcome and the intracellular replication of *C. neoformans* (Alanio et al. 2011).

Received: August 2, 2022. **Accepted:** September 13, 2022
© The Author(s) 2022. Published by Oxford University Press on behalf of FEMS. This is an Open Access article distributed under the terms of the Creative Commons Attribution License (http://creativecommons.org/licenses/by/4.0/), which permits unrestricted reuse, distribution, and reproduction in any medium, provided the original work is properly cited.

Cryptococcus neoformans is able to survive and even thrive in the acidic and proteolytic phagolysosome, its primary location when ingested by host macrophages (De Leon Rodriguez et al. 2018, Fu et al. 2018). The three potential outcomes of the ingestion of *C. neoformans* by host macrophages are host killing of the fungal pathogen, intracellular fungal replication or egress of the fungi from the host macrophage by lytic or nonlytic exocytosis (Zhang et al. 2015, DeLeon-Rodriguez and Casadevall 2016). Nonlytic exocytosis is the ability of the yeast to escape from its host macrophage with both host and pathogen remaining viable (Alvarez and Casadevall 2006, Ma et al. 2006), and this phenomenon has been shown to occur *in vivo* in mice (Nicola et al. 2011) and zebra fish (Bojarczuk et al. 2016). Initially, the three types of nonlytic exocytosis were classified as: type I, the complete extrusion of fungal burden from the host macrophage; type II, the partial expulsion of the fungal burden with at least one yeast remaining; and type III, the cell-to-cell transfer of one or more *C. neoformans* cells between host macrophages (Stukes et al. 2014, 2016). However, recent work has established that cell-to-cell transfer is the result of a sequential nonlytic exocytosis event followed by phagocytosis of an adjoining cell, a process termed 'dragotcytosis' (Dragotakes et al. 2019). Thus, the mechanisms for nonlytic exocytosis remain poorly understood, however, there has been an increasing body of evidence that it may be an important factor in *C. neoformans*–macrophage interaction.

There is considerable evidence that intracellular *C. neoformans* residency actively modulates the physiology of macrophages. In this regard, early studies showed that polysaccharide-laden vesicles that appeared to bud from cryptococcal phagosomes accumulated in the macrophage cytoplasm (Feldmesser et al. 2000). Phagosomal membranes become leaky with time (Tucker and Casadevall 2002, De Leon Rodriguez et al. 2018), reflecting damage from secretion of phospholipases and enlargement of the capsule (De Leon Rodriguez et al. 2018). Intracellular residence is associated with impairment of mitochondrial function and activation of cell death pathways (Coelho et al. 2015). *Cryptococcus neoformans* affects host cell NF-κB expression (Hayes et al. 2016), actin cytoskeleton dynamics (Johnston and May 2010), phagosomal pH (Fu et al. 2018, Dragotakes et al. 2020), and gene transcription profiles(Subramani et al. 2020) through mechanisms that are poorly understood, but are likely to reflect effects of cryptococcal products, which interfere with host cell physiology. In this regard, *C. neoformans* has recently been shown to release small molecules that affect macrophage function (Bürgel et al. 2020). *Cryptococcus neoformans* is known to release numerous proteins into the exterior of the cell (Chen et al. 1996, Geddes et al. 2015), some of which are released in extracellular vesicles (EV; Rodrigues et al. 2008). The mechanisms by which *C. neoformans* modulate and damage macrophages are poorly understood, but are likely to reflect effects of cryptococcal products on host cell physiology. In this study, we investigated whether *C. neoformans* released proteins into macrophage-like J774.1 immortalized cells. The results show that *C. neoformans* infection of macrophage-like cells is followed by the production of numerous proteins, including a Yeast Oligomycin Resistance (Yor1) protein, an ATP binding cassette transporter (ABC transporter) whose deletion affects the frequency of nonlytic exocytosis.

Results

Approaches to study *C. neoformans* proteins secreted during infection of murine macrophages

To demonstrate the presence of cryptococcal proteins in macrophages, the first approach we attempted was to radioactively label the proteins of *C. neoformans*, then add these labeled-fungi to macrophages for phagocytosis and analyze whole coinfection lysates for the presence of radioactive proteins. Hence, we grew *C. neoformans* with different concentrations of ^{35}S-methionine and ^{35}S-cysteine. We observed normal growth curves in different concentrations of radiolabeling material (Fig. 1A). Next, we analyzed the labeling efficiency of *C. neoformans* and determined that H99 strain grown in the presence of 20 μCi ^{35}S-Met and ^{35}S-Cys during a 4-hour incubation yielded the greatest labeling efficiency (Fig. 1B). We then infected J774.16 macrophages with radiolabeled *C. neoformans*, lysed the infected murine cells, and subsequently run whole cell lysates on a 2D isoelectric focusing apparatus. This revealed that detectable amounts of radiolabeled-fungal proteins were released into the J774.16 macrophages. Further, the protein profile was different from that observed in a lysate of *C. neoformans* grown in Sabouraud media (Fig. 1C). Having established that fungal proteins can be identified from co-cultures of *C. neoformans* infected J774.16-macrophages, and with the goal of identifying the secreted fungal proteins via proteomic mass spectroscopy, we attempted nonradioactive methods of protein labeling. First, we attempted to label newly synthesized cryptococcal proteins by growing fungi in the presence of tRNA precharged with biotinylated lysine, but observed no cryptococcal labeling (data not shown). Second, we attempted click-chemistry by labeling nascent proteins with L-Homopropargylglycine (HPG), a glycine analogue containing alkyne moiety that can be subsequently click-labeled. Again, we were unable to observe detectable labeled-protein bands, despite the fact that the mammalian Jurkat cells, used as a positive control for click-chemistry, did yield distinct, click-labeled protein (data not shown). We then attempted to isolate fungal-phagosome isolation, without success. Although we do not have explanation as to why tRNA charging and click-chemistry failed, we suspect that these reflect peculiarities specific to the cryptococcal system. The failure to isolate intact *C. neoformans*-containing phagosomes by the well-tried magnetic bead technique, so successful when applied to bacterial phagosomes, may simply reflect the large size of the cryptococcal phagosome, and the fact that *C. neoformans* phagosomal membranes are damaged during the intracellular infection process (Tucker and Casadevall 2002). The large size of the phagosome can leave the membrane vulnerable to shear forces and accentuated by *C. neoformans*-driven membrane damage (De Leon Rodriguez et al. 2018). We decided to resort to a selective extraction protocol.

Cryptococcus neoformans protein profile

Given that the capsule and cell wall confer upon fungal cells a tremendous structural strength that requires harsh methods for extracting proteins relative to those required for lysing macrophage-like cells, we reasoned that we could lyse and extract proteins from the host cells while leaving internalized *C. neoformans* cells intact. Consequently, we devised and tested a protein extraction protocol designed to extract all host J774.16 proteins, which would not lyse and extract fungal intracellular

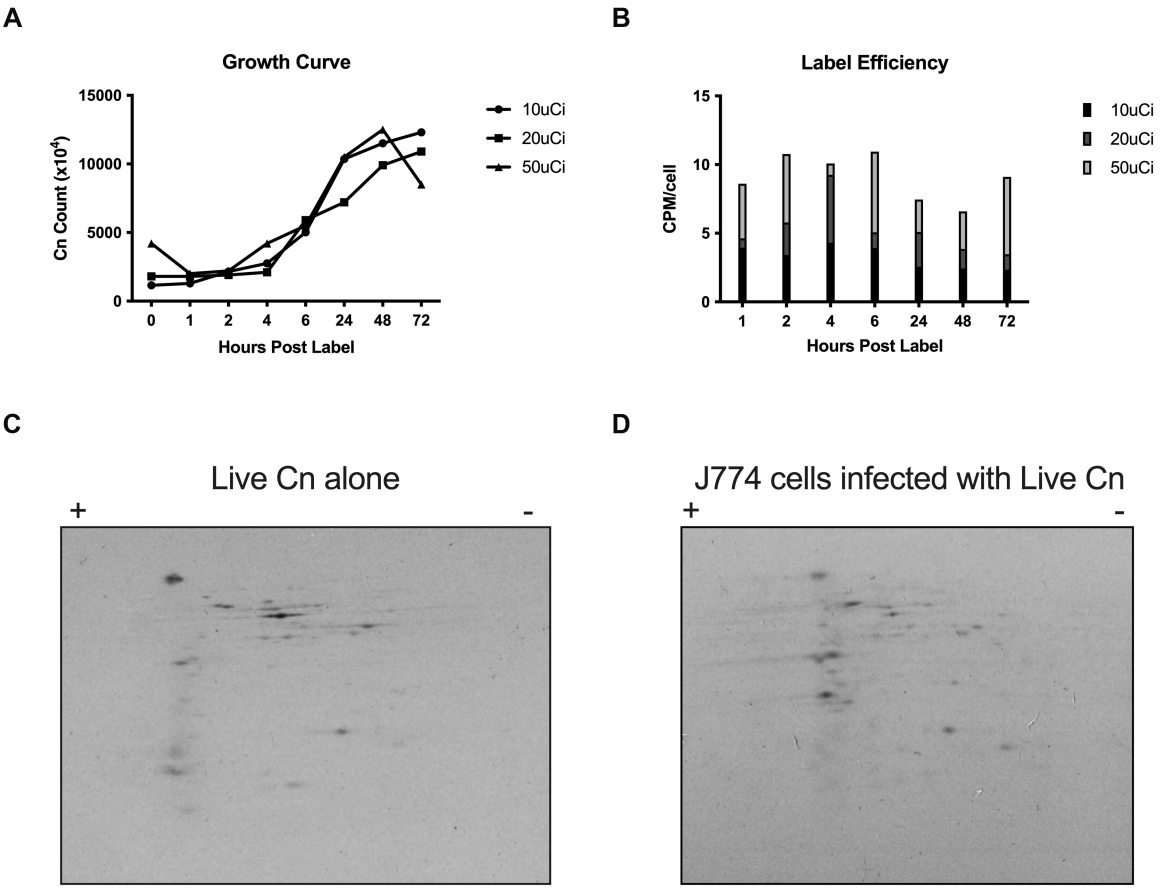

Figure 1. Radiolabeling *C. neoformans* proteins to detect putatively secreted proteins during mammalian infection. (A)^{35}S labeling does not affect growth of *C. neoformans*. Growth was measured after addition of ^{35}S-methionine and -cysteine to Sabouraud broth, at 30°C with constant agitation, at different time points over 72 h. (B) *Cryptococcus neoformans* incorporates ^{35}S-amino acids. CPM measurements were made for each of the ^{35}S labeling conditions by sampling at each time point. to calculate CPM/cell was calculated by (total CPM)/(total cell count). Shown is the mean CPM/cell for each time point. We determined 20 μCi and 4 h of incubation to yield maximum label and minimizing excess radiation for subsequent experiments. (C) and (D) As a proof of concept for efficient cryptococcal labeling and identification of putatively secreted proteins during infection, we labeled *C. neoformans* with ^{35}S, and prepared protein lysates from broth culture and from infected J774.16 murine macrophage-like cells, followed by extraction of proteins from the coculture and then run in a 2D gel. Experiment shows the opportunity for isotopic labeling of amino acids to detect differentially expressed proteins during host–pathogen interactions.

proteins. This protocol would allow proteins secreted by *C. neoformans* to be coextracted within the mammalian cell lysates and their identity distinguishable by computational proteomic analysis. First, we subjected live *C. neoformans* cells in the absence of macrophages to a widely used mammalian lysis process which consists of multiple rounds of passaging through a 26 G needle; this process yielded no identifiable cryptococcal proteins. Hence, the isolation process used did not release proteins from *C. neoformans* viable cells. Having established a lysis and proteomics protocol, we infected J774.16 macrophages with live fungi from an H99 fungal strain (live H99); as a control, J774.16 macrophages were infected with heat-killed (HK) H99 (HK H99), reasoning that no active secretion is occurring in HK-H99 and the identified proteins would instead derive from macrophage-degradation of fungal remnants. We identified 127 cryptococcal proteins in lysates of J774.16-macrophages infected with live H99 and 117 proteins from macrophages infected with HK H99. The cryptococcal proteins extracted from macrophage-like cells containing live compared to HK *C. neoformans* had only 8% (18/226 proteins) proteins in common (Fig. 2 and Table 1; Table S1, Supporting Information), supporting our rationale. Among the 109 proteins identified in lysates of macrophages that had ingested live *C. neoformans* was urease, a known secreted virulence factor, among others such as transaldolase and phospholipase D (PLD) , which are less characterized but could conceivably be secreted. To extract information on these proteins, we took advantage of available bioinformatic analysis to predict transmembrane domains and signal sequences. Of these fungal proteins, 19 proteins are predicted to have a signal sequence according to at least one of the three tools and 39 have at least one transmembrane domain (Table S1, Supporting Information). Other secretion mechanisms are possible, in particular EV secretion. Using the recently established database for EV proteins of fungi, ExVe (http://exve.icc.fiocruz.br/), we analyzed whether the proteins identified were previously identified as secreted via association with EVs (Table S1, Supporting Information). Of the cryptococcal proteins identified in our proteomic analysis 23% (51/226) were previously detected as EV-associated. For the purposes of this report we did not analyze the host proteins.

Identification of new virulence factors in *C. neoformans*

To validate that our strategy could identify novel fungal virulence factors, we then performed a preliminary analysis of putative novel virulence factors. Among the proteins identified in

Figure 2. Proteomics analysis detected different cryptococcal proteins when J774.16 cells were infected with live Cn versus HK Cn. Using spectral count as a method of semiquantitative expression levels, we identified 127 from live *C. neoformans* and 117 cryptococcal proteins from HK *C. neoformans*, with little overlap between identified proteins. Full list of proteins in Table S1 (Supporting Information); transcriptional comparisons in Table S2 (Supporting Information).

Table 1. Top 10 *C. neoformans* proteins identified in J774.16 macrophage infected with live H99.

Gene	Protein (length)	Molecular weight (KDa)	Spectral count	Features	Comments
CNAG_01984	Transaldolase (324 aa)	35	24.407		Role in CN virulence is unknown. Involved in resistance to nitric oxide (NO; Missall et al. 2006), which may aid CN intracellular survival.
CNAG_06812	Phospholipase D (1745 aa)	196	13.054		Role in CN virulence is unknown. Unlike Plp1, not detected as secreted in culture (Chen et al. 1997)
CNAG_05894	Dynein heavy chain 1, cytosolic (4630 aa)	524	10.331		Transport (via GO)
CNAG_03655	Hypothetical protein (2007 aa)	222	9.2767		43% homology to S. cerevisiae *Num1p*, which is involved in organelle migration
CNAG_04172	Transcription factor C subunit 6 (826 aa)	91	6.7986		Transcription/translation
CNAG_02103	Hypothetical protein (1896 aa)	209	6.4459		Homologs in other fungi but no function prediction
CNAG_00583	Hypothetical protein (1109 aa)	118	6.4459	1 TM	No significant homology detected
CNAG_06332	Hypothetical protein (1093 aa)	121	5.8274		No significant homology detected, increased virulence (Gerstein et al. 2019)
CNAG_06728	Kinesin (958 aa)	107	4.8814		Transport
CNAG_06818	Hypothetical protein (837 aa)	93	4.2973		Likely homology to Hap1 of *Saccharomyces cerevisiae* (Jung et al. 2010)
CNAG_07781	ATP-dependent bile acid transporter (1618 aa)	180	4.2973	13 TM	Transport
CNAG_04370	U3 small nucleolar RNA-associated protein 10 (2022 aa)	222	4.2973	SP	Ribosomal processing

TM = transmembrane domain predicted, SP = signal peptide predicted.

macrophage-like cells infected with live *C. neoformans* was the ABC transporter Yor1, with thus far unknown roles in virulence. Yor1 (J9VQH1) has been identified as secreted via association with EVs (Rizzo et al. 2021).

To study its role in fungal biology and virulence, and validate our screening strategy, we studied both a deletion strain from an available deletion library, generated by Madhani laboratory (*yor1*Δ), as well as generated *de novo Yor1*-deleted strains of *C. neoformans*, resorting to well-established replacement with *URA5*-selection cassette and biolistic particle delivery to remove the coding sequence of *Yor1* (Figure S1, Supporting Information). Screening with colony-PCR identified three independent *yor1*Δ strains (*yor1*Δa-c). For the *de novo* deletion strains generated, we characterized virulence factors, such as melanin production, virulence in *Galleria mellonella*, capsule size in minimal media (MM), cell body size, capacity to alter phagosomal pH, urease

activity, and growth rates (Figures S2–S5, Supporting Information). To evaluate whether *Yor1* deletion was associated with decreased melanization, we grew the *C. neoformans yor1*Δ strain from the 2008 Madhani knockout library, the three independently generated *yor1*Δ*a*, *yor1*Δ*b*, and *yor1*Δ*c*, and their parental strains H99W and H99, respectively, in MM containing L-DOPA. These growth conditions normally induce melanization (Figure S2, Supporting Information). Following 3 days of growth at 30°C, there is a notable defect in melanization in both sets of *yor1*Δ mutants, with the notable exception of *yor1*Δ*c* which exhibits wild-type melanization.

To assay whether *Yor1* was involved in virulence of *C. neoformans*, we used the *G. mellonella* wax moth model of infection (Figure S3, Supporting Information). We observed that *yor1*Δ strain from the 2008 strain library had reduced virulence compared to the parental strain from the library (H99W). For *yor1*Δa and *yor1*Δb, there was a similar reduction in virulence. Strain *yor1*Δc displayed different phenotypes than its counterparts *yor1*Δa and *yor1*Δb, which may be due to spurious secondary mutations in this strain, albeit we did not investigate this further. Overall, in three of four deletion strains Yor1-deletion was associated with reduced melanization and virulence in wax moth.

We detected a reduction in capsule size in *yor1*Δ strains in MM, but this was dependent on parental background (Figure S4, Supporting Information). Thus, it is possible that Yor1 is involved in capsular synthesis, secretion, or assembly, albeit this is dependent on strain background. We had previously associated capsule changes and urease production with capacity to manipulate phagolysosomal pH (De Leon-Rodriguez et al. 2018, Fu et al. 2018). Given previous association of *Yor1* with transport of organic anion transport, we posited that *Yor1* could contribute to cryptococcal manipulation of phagosomal pH (Figure S4, Supporting Information). We found that Yor1 is not involved in manipulating phagolysosomal pH. To assess any growth defects in *yor1*Δ, we performed growth curves in liquid media over the course of 72–96 h (Figure S5, Supporting Information). When analyzing cultures grown in Sabouraud or MM, we observed no growth defects: a similar lag phase duration, slope of log phase, and establishment of stationary phase. As urease activity is required for optimal growth at host pH in *C. neoformans* (Fu et al. 2018), we assessed urease activity in *Yor1*-deletion strains, and found no changes (Figure S5, Supporting Information).

We also evaluated rates of nonlytic exocytosis *in vitro* of *yor1*Δ strains when exposed to bone marrow-derived macrophages (BMDMs). J774.16 cells were not used as their high motility is challenging for nonlytic exocytosis quantification. We infected BMDMs with *yor1*Δ strains and wild-type H99 (Fig. 3) and measured nonlytic exocytosis rates in three, independent 24 h time-lapse movies with BMDMs infected with wild-type H99 with 50–100 cells tracked per individual movie. We observed a mean nonlytic exocytosis rate reduction in all *yor1*Δ strains. The different parental backgrounds of deletion strains may generate some variability, but overall the defects are the same. Although we were not able to complement the *yor1*Δ strains, we note that the reduced nonlytic exocytosis phenotype was observed with four independent mutants, which provides confidence for a causal association. A search in available data, via FungiDB, and ClustalOmega, showed that other strains of *C. neoformans* have a copy of *Yor1*, with a close homologue (CNBG_2112) in *C. gattii* strain R265. These searches also identified that *Yor1* is upregulated after incubation in DMEM, 5% CO_2 (see Figure S6, Supporting Information). We also found that *Yor1* was transcriptionally up-regulated in experimental models of rabbit cryptococcal meningitis (Yu et al. 2020). To assess the integrity of the library strains for a nonspecific defect that affected nonlytic exocytosis, and thus if genetic manipulation of fungi could affect nonlytic exocytosis, we analyzed the *cir1*Δ (CNAG_04864), a strain known to have defects in iron acquisition, which causes defects in virulence (Jung et al. 2006), and ascertained that despite known defects in virulence, the rate of nonlytic exocytosis of *cir1*Δ is comparable to that of the wild-type H99 strain (data not shown).

Given the lack of known functions of Yor1, and our data suggesting that Yor1 is secreted in association with EVs, we posited whether Yor1 may affect EV secretion. To analyze EV profile and whether this is affected by *Yor1*, we performed a Nanoparticle Tracking Particle analysis (NTA; Reis et al. 2021). We observed that Yor1 deletion led to changes in size profile of EVs when compared to parental strains (Fig. 4). However, we did not observe a significant change in number of secreted EVs. Our data suggests that Yor1 affects composition, formation, and/or release of EVs.

Discussion

This study investigated *C. neoformans* proteins in macrophages after fungal cell ingestion in macrophage-like cells. The study was prompted by recent evidence that intracellular residence of *C. neoformans* in macrophage-like cells is associated with changes to host cell physiology and metabolism (Coelho et al. 2015), which presumably reflect host cell damage and/or modulation by the fungal cells. Proteins secreted by human pathogenic fungi during macrophage interaction *in vivo* has been determined before for *Candida albicans* (Kitahara et al. 2015) and *Aspergillus fumigatus* (Schmidt et al. 2018), but not for the *C. neoformans* species complex. We focused on developing a protocol to identify putatively secreted proteins, as those may have direct effects in modulating host cells and are usually major virulence factors and/or immunogens. The major finding in our study is that *C. neoformans* intracellular residence is associated with the production of a variety of protein products and some of these proteins have important roles in virulence and pathogenesis.

Cryptococcus neoformans protein secretion in macrophage-like cells was established by two independent approaches. First, we show, by 2D protein electrophoresis after phagocytosis of ^{35}S-labeled *C. neoformans* cells, that a new set of fungal proteins is discernible in host cells lysates, presumably by secretion of fungal proteins during mammalian infection (Fig. 1C and D). Second, we used mass spectroscopy to identify fungal proteins coisolated in macrophage lysates that ingested live or killed *C. neoformans* to identify the secreted proteins of *C. neoformans*.

The protein sets identified in J774.16 macrophage-like cells that ingested live or dead *C. neoformans* cells were different. This provides strong support for the hypothesis that the proteins isolated from macrophage-like cells that ingested live *C. neoformans* cells were produced and secreted by live fungal cells while inside the macrophage and was not the result of macrophage digestion of fungi. Regardless of secretion, the coisolation and identification in mammalian lysates, strongly indicates these proteins are produced in high levels *in vitro* during mammalian infection. These fungal proteins identified within infected macrophage-like cells could be located at the cryptococcal phagosomes and/or the cytoplasm, given that cryptococcal-phagosomes macrophages are leaky (Tucker and Casadevall 2002, De Leon Rodriguez et al. 2018). We found no overlap with proteins previously identified in cryptococcal secreted proteins (Geddes et al. 2015) or with the first description of extracellular vesicles (Rodrigues et al. 2008). However, we found that using the ExVe database (http://exve.icc.fiocruz.br/; Parreira et al. 2021) we found that several of the

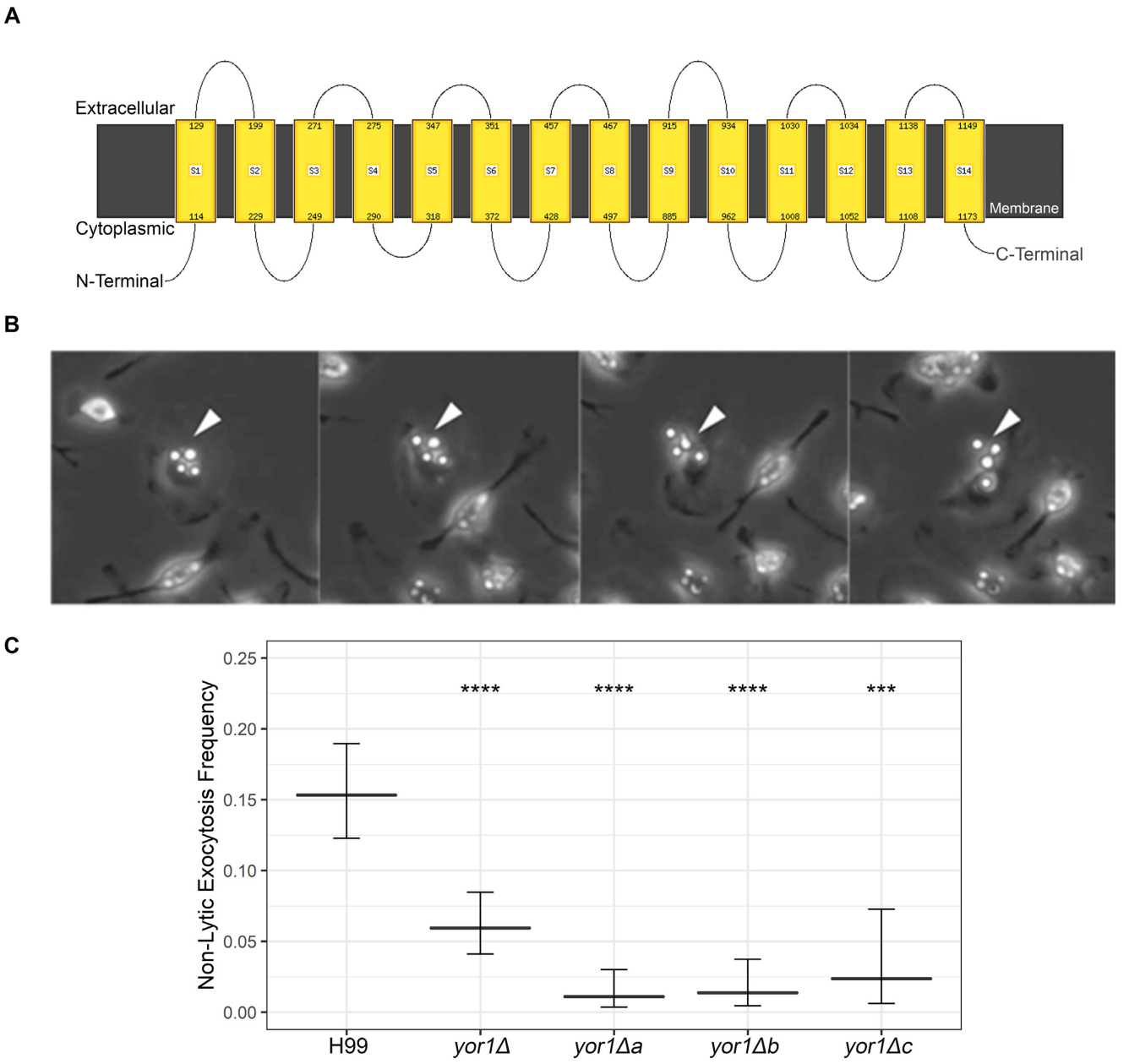

Figure 3. Yor1, a transmembrane protein, affects nonlytic exocytosis of *C. neoformans*. (A) Schematic of Yor1, showing transmembrane domains, as predicted by bioinformatic tool Phyre2. (B) H99 and *yor1*Δ-strains were opsonized with mAb 18B7 prior to phagocytosis by 7-day-old BMDMs from C57Bl/6 mice. After time-lapse microscopy at 10× magnification for 24 h, each macrophage was tracked for nonlytic exocytosis (white arrows). (C) Strains with *yor1*Δ as well as each of three *de novo* mutant strains show a defect in nonlytic exocytosis compared to wild-type strain H99. Comparisons were performed with a two-tailed test of equal proportions compared to the wild-type H99 strain with Bonferroni correction for multiple tests. *** and **** signify $P < .001$ and .0001, respectively. Error bars denote 95% confidence intervals.

proteins in our dataset were identified by other groups as secreted in and/or associated with EVs. This provides confidence that these proteins can be found on the outside of cryptococcal cells. Our result is a proof-of-concept, establishing the release of a protein set in macrophages and anticipate that future work will expand and further define this set, such as the very recent publication using a total lysate of murine macrophages and *C. neoformans* (Sukumaran et al. 2022). We do not claim a comprehensive protein export set, as differences in experimental conditions, proteomic analysis, bioinformatic pipelines, and recent advances in proteomics is likely to significantly affect these datasets, and reproducibility between proteomics experiments is known to be often unsatisfactory due these variables (Karpievitch et al. 2010).

Cryptococcal proteins isolated from macrophage-like cells containing live *C. neoformans* cells included some the well-known virulence factors such as urease Ure1 (Cox et al. 2000, Singh et al. 2013, Fu et al. 2018), as well as Zsd3 (Li et al. 2011), but the large majority of proteins identified were either previously not implicated in virulence or were hypothetical proteins due to significant divergence to known proteins. Urease is required for brain dissemination of *C. neoformans* and well-known for being secreted (Cox et al. 2000, Singh et al. 2013, Fu et al. 2018). Urease activity prevents

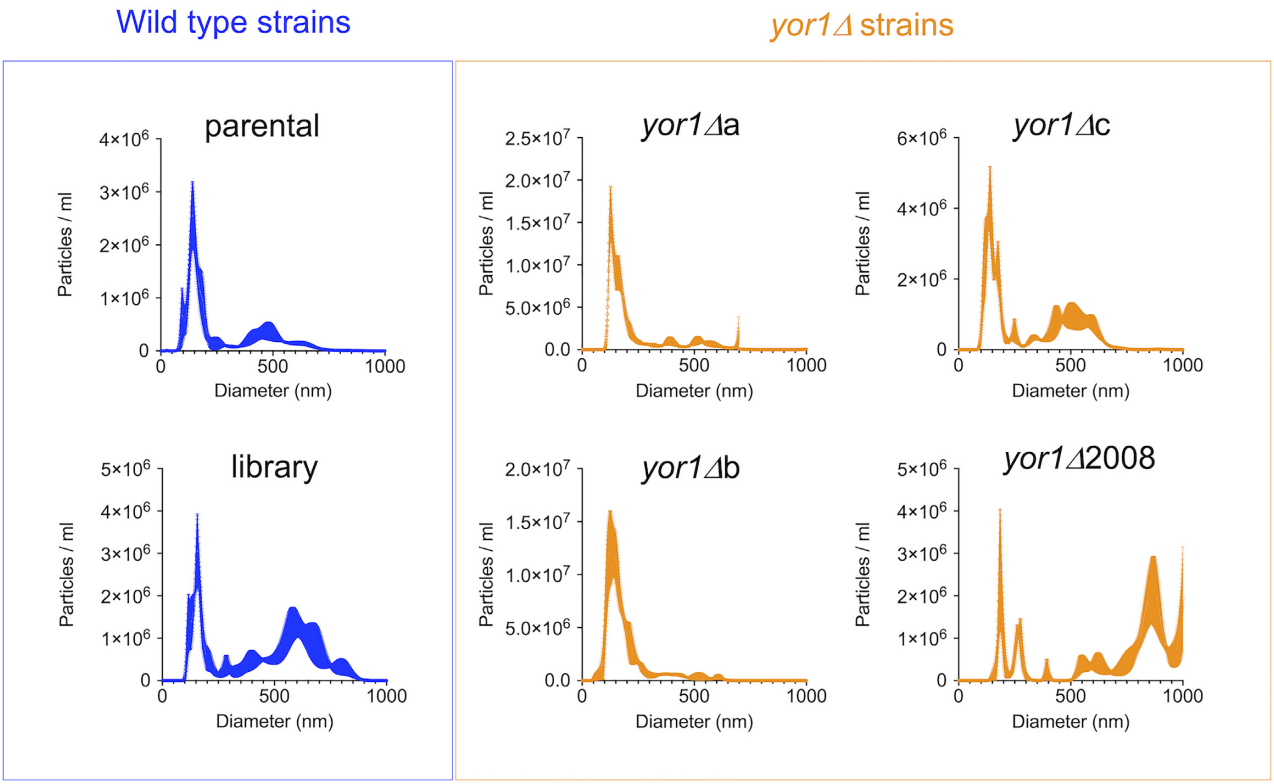

Figure 4. *Yor1* deletion leads to a change in EV size distribution. EVs were analyzed via NTA. Representative plots are shown.

acidification of fungal-containing phagolysosomes, and is required for optimal growth at mammalian pH (Fu et al. 2018). We also identified PLD. Whereas phospholipase B is a well-characterized virulence factor in *C. neoformans* pathogenicity (Cox et al. 2001, Noverr et al. 2003, Djordjevic 2010, p. 1) that was recently implicated in mediating damage to the membrane of phagolysosomes containing *C. neoformans* (De Leon Rodriguez et al. 2018), PLD has not been implicated in virulence thus far. Previous analysis of *C. neoformans* supernatants obtained in microbiological media supplemented with egg yolk revealed no PLD activity (Chen et al. 1997). It is interesting that the gene encoding for PLD, CNAG_06812, is located in the alpha mating locus, which is associated with virulence (Sun et al. 2020). Expression of this protein inside macrophages could mediate damage to the phagosomal membrane in a manner similar to PLB1(De Leon Rodriguez et al. 2018), and may contribute for the association the alpha mating locus with virulence in *C. neoformans*. These hypotheses remain to be tested. Another protein potentially associated with virulence present in macrophage-like cells was Transaldolase (Tal1). While the function of Tal1 in *C. neoformans* virulence has not been widely studied, there is evidence for its role in resistance to nitric oxide, which could contribute to fungal cell survival in macrophage-like cells (Missall et al. 2006). We note that a large proportion of the peptides identified belong to so called 'hypothetical proteins' identified in the *C. neoformans* genome. Further, we found that a large amount of these proteins were differentially regulated during experimental infection: 100% of proteins were also reported to be differentially expressed in CSF of corticosterone-treated rabbits and infection of macrophages (Yu et al. 2020), and frequently found to be expressed during experimental virulence studies. Our data strongly suggests that these hypothetical proteins are expressed during infection and *in vivo*, providing fertile ground for new investigations into their function in the physiology and virulence of *C. neoformans*.

Among the proteins found in macrophage-like cells infected with live *C. neoformans* was the ABC transporter Yor1, a homologue of Yor1 protein in *S. cerevisiae*. Yor1 and other ABC transporters have a variety of roles in other organisms, but one overarching theme is the translocation of solutes across membranes, which can include polysaccharides, peptides, ions, and lipids (Cangelosi et al. 1990, Henderson and Payne 1994, Decottignies et al. 1998, Davidson and Chen 2004, Kihara and Igarashi 2004, Nishida and Tsubaki 2017, Kumari et al. 2021). ABC transporters are characterized by multiple transmembrane domains and an ATPase-domain; in microbes, this family has an enormous array of functions ranging from iron or nutrient import (Henderson and Payne 1994, Kumari et al. 2021) to the export of virulence factors such as capsular polysaccharide (Orsi et al. 2009). In *S. cerevisiae*, Yor1 influences the cell membrane composition by translocating phosphatidylethanolamine outwards (Khakhina et al. 2015), and is necessary in efflux of beauvericin, a microbial product, which potentiates activity of antifungal drugs (Shekhar-Guturja et al. 2016). In *C. albicans*, Yor1 is required for efflux of geldanamycin, a Hsp90 inhibitor (Hossain et al. 2021), and has been implicated in antifungal resistance in *C. lusitaniae* (Reboutier et al. 2009), but its role in cryptococcal homeostasis and host–pathogen interactions has not been studied. Yor1 is likely enmeshed in cellular membranes, but efforts to perform fluorescent localization were unsuccessful. Since the role of Yor1 in *C. neoformans* physiology was unknown, we performed some exploratory assays with *yor1*Δ strains, including interaction with mammalian cells. We observed no difference in growth rates in microbiological media, but detected alterations in capsular size in MM and a decrease in melanin secretion in *yor1*Δ deletion strains, with some alterations in EV size distribution pattern, suggesting that it may be involved in export

of (some) virulence factors and/or EV formation and packaging. The role of Yor1 in differential packaging of EV content was not tested. Analysis of the frequency of nonlytic exocytosis for *C. neoformans* strains deficient in Yor1 revealed reduced rates of fungal cells exiting macrophage-like cells. Thus, Yor1 is involved in transport of still unknown moieties that affect proteins or lipids needed for secretion of certain subset of virulence factor-carrying EVs, which overall increase melanin secretion and capacity to provoke nonlytic exocytosis. This is also linked with enhanced capacity to kill wax moth larvae.

In summary, we report a new method to investigate proteins secreted by microbes ingested by macrophages. We reason that this protocol may be extended to other systems and even *in vivo* in animal models. We show that ingestion of live and dead *C. neoformans* cells by macrophage-like cells results in release of different protein sets, consistent with active release and digestion of fungal cells, respectively. The finding that some of these proteins modify the course of *C. neoformans* intracellular pathogenesis is consistent with recent findings that fungal cells actively modulate some processes such as nonlytic exocytosis and cell-to-cell transfer (dragotcytosis; Dragotakes et al. 2019), and can even reprogramme immune response in macrophages (Dang et al. 2021) The discovery that many of the proteins putatively secreted into macrophage-like cells are poorly characterized provides a rich trove of new research avenues that could reveal fundamentally new processes in intracellular *C. neoformans* pathogenesis.

Materials and methods

Strains

H99 (Serotype A) fungal cells from frozen stocks (10% glycerol) were plated on rich Sabouraud agar plates with single colonies subsequently picked and maintained in Difco™ Sabouraud Dextrose Broth (BD, Sparks, MD) at 30°C with agitation for 18 h. Our initial screens were conducted with a mutant library generated by Drs Hiten Madhani and Suzanne Noble at University of California San Francisco and made publicly available at Fungal Genetic Stock Center. The library included parental H99 and approximately 2000 gene knockouts (Liu et al. 2008). The strain used for *de novo* mutant generation is a derivative of H99, H99-FOA with a URA5 selectable marker (Edman and Kwon-Chung 1990).

Cryptococcus neoformans protein isolation

Cryptococcal protein isolation was accomplished by adding equal parts prewashed (with ice-cold PBS with protease inhibitors), H99 and 0.5 mm Zirconia/Silica Beads (Biospec, Bartlesville, OK) to a microcentrifuge tube and vortexing at max speed for 4 cycles of 5 min agitation, 2 min on ice. The lysate was centrifuged, 4000 × *g* at 4°C for 5 min and the supernatant was removed and sequentially centrifuged three times to remove cellular debris, intact *C. neoformans* and beads while leaving proteins in the resulting supernatant.

Macrophage-like cell lines

J774.16 is a murine macrophage-like cell line. From frozen stock, J774.16 cells were washed several times to remove freezing media and plated on noncell culture-treated dishes. They are maintained in DMEM (Gibco), 10% NCTC-109 medium (Gibco), 10% heat- inactivated FBS (Atlanta Biologicals), and 1% nonessential amino acids, at 37°C with 9.5% CO_2. For infection, macrophage-like cells from anywhere between passages 4 and 10 are plated at ∼60% confluency on 150 mm noncell culture-treated dishes (Corning® #430597) and activated with 150 U/ml interferon gamma and 10 ng/ml lipopolysaccharide overnight. Infection is accomplished under the same conditions with the addition of 10 μg/ml of 18B7 (an opsonic monoclonal antibody against *C. neoformans*' polysaccharide glucuronoxylomannan capsule) for 2 h (Casadevall et al. 1998).

BMDM isolation, differentiation, and infection

All animal experiments were approved by Johns Hopkins University IACUC under protocol number MO18H152. Primary BMDM cells were used to study nonlytic exocytosis. These cells were isolated from 6 to 8-week-old C57Bl/6 female mice. BMDM were differentiated from bone marrow at 37°C with 9.5% CO_2 for 7 days. BMDM media consists of DMEM, 20% L929 conditioned media, 10% FBS, 1% nonessential amino acids, 1% GIBCO™ GlutaMAX™, 1% HEPES, 1% penicillin–streptomycin, and 0.1% β-mercaptoethanol. After 7 days, the differentiated BMDMs were detached using Cell-Stripper™ (Corning, Corning, NY) and 10^4 BMDMs were plated on MatTek™ dishes, which have a central glass coverslip insert in the center of a hollowed polystyrene plate and allows for time-lapse microscopy. Fungal strains were counted and opsonized with 18B7 at an MOI of 3:1 for 2 h at 37°C and 9.5% CO_2. After 2 h infection, the plates were washed three times with BMDM media for subsequent 24 h time-lapse microscopy at 37°C and 9.5% CO_2 and nonlytic exocytosis analysis.

Nonlytic exocytosis assay

Wild-type or *yor1*Δ strains were resuspended and opsonized with 18B7 (monoclonal antibody against the capsular polysaccharide of *C. neoformans*) to infect at MOI of 3:1 for 2 h at 37°C and 9.5% CO_2. After 2 h infection, the plates were washed three times with BMDM media for subsequent 24 h time-lapse microscopy at 37°C and 9.5% CO_2. Images were acquired in a Axiovert 200 (Zeiss, Oberkochen, Germany) and a Hamamatsu ORCA ER cool charged-coupled device (CCD) with a heated chamber and supplemental CO_2 were used for all time-lapse microscopy. Time-lapse microscopy was done at 10x bright-field with an image captured every 4 min for 24 h. Time-lapse was compiled in ImageJ and 50–100 infected macrophage-like cells were tracked through the course of 24 h. Type I nonlytic exocytosis was counted when all yeasts were expelled from the host macrophage with both remaining intact. Type II was counted when part of the fungal burden was expelled while a portion remained within the host macrophage. Type III, or cell-to-cell transfer, was counted when an infected BMDM would pass one or more yeast directly to another BMDM. Infected macrophage-like cells that underwent lytic exocytosis were marked as lysed.

Protein isolation from *C. neoformans*-infected macrophage-like cells

Plates, 10 cm, with monolayers of approximately 2.0 × 10^7 *C. neoformans*-infected J774A.16 macrophage-like cells or BMDM, were rinsed with warm PBS to remove noninternalized fungus and unattached dead macrophages. After scraping the remaining infected macrophage-like cells from the plate, they were centrifuged at 1000 × *g* for 5 min at 4°C to pellet the infected macrophage-like cells. The supernatant was discarded and the pellets were resuspended in ice-cold water containing cOmplete™ protease inhibitors (Roche). Each sample was subsequently passed 10 times through a 26-gauge needle to shear the host macrophage-like cells while leaving the fungi intact. Visual inspection under a microscope confirmed macrophage lysis while fungal counts confirmed

the viability of *C. neoformans* through the lysis procedure. Most *C. neoformans* and cellular debris was removed from the lysate by an initial centrifugation of 3000 × *g* for 10 min at 4°C. A total of two subsequent 8000 × *g* centrifugations of the resulting supernatants for 10 min at 4°C removed all cellular debris and remaining *C. neoformans*. Proteins were concentrated in a Savant Speed Vac Concentrator. Total proteins were quantified using Pierce™ BCA Protein Assay Kit (ThermoFisher Scientific). A total of 50 μg of each total lysate (mixture of murine and cryptococcal proteins) from the protein isolation step was run on a 12% NuPAGE™ tris-acetate gel (Thermo Fisher Scientific) 2 cm into the gel prior to Coomassie R250 staining and water destaining for subsequent proteomic analysis.

Proteomics

Resulting gel lanes containing a mixture of fungal and mammalian proteins were excised and fractioned into 1–5 sections prior to in-gel protein digestion and were analyzed on an Orbitrap Fusion™ Tribrid™ (Thermo Scientific) mass spectrometer at the Herbert Irving Comprehensive Cancer Center (Columbia University Medical Center) proteomics facility by Dr Emily Chen. Experiment was performed once. Databases were downloaded from Uniprot and Sequest HT from Proteome Discoverer 1.4 was used to search data. Peptide data was aligned and filtered using murine and cryptococcal (H99, Broad Institute; Janbon et al. 2014) databases. Mass spectrometry proteomics data have been deposited to the ProteomeXchange Consortium via the PRIDE (Perez-Riverol et al. 2019) partner repository with the dataset identifier PXD024951. Spectral counts counts in Table S1 (Supporting Information) .

Generation of *de novo* deletion strains

Flanking regions of 1 kb to the genomic sequence of *YOR1* (CNAG_03503) and the selection marker, *URA5*, were amplified by PCR to contain overlapping nucleotides for a 2-step fusion PCR. For step 1, *YOR1* was amplified from *C. neoformans* genomic DNA as a template; *URA5* was amplified from plasmid DNA containing the *C. neoformans* actin promoter and the coding sequence for *URA5* (Table S2, Supporting Information). All primers contained annealing overhangs for subsequent fusion PCR. After gel purification of all PCR products, the second step of fusion PCR yielded a complete sequence including the 5′ 1000 bp region of genomic *YOR1*, *URA5* selectable marker and the 3′ 1000 bp region of genomic *YOR1*. This combined fusion PCR product was purified in preparation for biolistic particle delivery.

Biolistic particle delivery and screening

The Bio-Rad PDS-1000 biolistic particle delivery system was used to replace *YOR1* in H99-FOA *C. neoformans*. H99-FOA is an auxotrophic mutant lacking the ability to grow without supplemental uracil and this strain was selected for its ease in knockout generation. Inserting *URA5* as a selection marker allows for transformants to grow without supplemental uracil. H99-FOA was grown to stationary phase overnight in rich YPD media at 30°C. After plating a lawn on 1 M sorbitol-YPD plates, the plates were dried in a sterile hood. The DNA preparation involves coating 10 μl of 0.6 μm Gold microcarriers (1652262 Bio-Rad, Hercules, CA) with 1 μg of purified DNA by gently vortexing DNA, 10 μl 2.5 M $CaCl_2$ and 2 μl 1 M spermidine-free base before washing with 100% EtOH. A volume of 10 μl of the DNA-coated microcarrier beads dried on 2.5 cm microcarrier discs (1652335 Bio-Rad). The manufacturer's protocol for operation of the PDS-1000 system was followed. Transformed plates were allowed to recover overnight at room temperature before subsequent streaking on rich media plates where isolates were selected. For screening of successful transformants, cells from 50 colonies were lifted and pooled in groups of 10. Successful replacement of *YOR1* was tested using colony PCR to amplify the *YOR1* locus. Successful transformants contained a shorter product with *URA5* (1.3 kb) replacing the endogenous *YOR1* gene (5 kb). A total of three de novo Δ*yor1* mutants were isolated were confirmed with single colony PCR and named *yor1*Δa, *yor1*Δb, and *yor1*Δc.

Characterization of *yor1*Δ mutants

To assess the cell body and capsule size of *yor1*Δ mutants versus wild-type H99, both strains were grown to stationary phase at 72 h at 30°C in MM composed of 15 mM dextrose, 10 mM $MgSO_4$, 29.4 mM KH_2PO_4, 13 mM glycine, and 3 μM thiamine-HCL with constant agitation. Liquid cultures were centrifuged at 4000 × *g* for 15 min to pellet the cells. The supernatant was saved for vesicle purification, and the pellet was resuspended in PBS for subsequent India ink negative stain imaging. Images were captured on an Olympus IX 70 microscope (Olympus America Inc., Melville, NY) to further compare mutants with wild-type H99. Cell body and capsule radius were measured using QCA, the custom cell body and capsule measurement application.

Melanization assay

Cryptococcus neoformans strains were grown overnight in YPD broth at 30°C until they were in stationary phase. Cultures were washed twice in PBS, and inoculated into MM at 10^6 cells/ml with 1 mM L-3,4-dihydroxyphenylalanine (L-DOPA). Cells were grown at 30°C and monitored daily for pigment formation. Cultures were imaged after 3 days.

Infection of *G. mellonella*

Final instar *G. mellonella* larvae were obtained from Vanderhorst Wholesale Inc., St. Marys, OH, USA. Healthy cream-colored larvae roughly between 175 and 225 mg were sorted and separated into groups of equal numbers. *Cryptococcus neoformans* strains were grown overnight in 1 ml of YPD broth until the culture was in stationary phase. Larvae were then infected with 10 μl of 10^7 *C. neoformans* cells/ml in a PBS suspension. Survival was measured daily over the course of 10 days, with survival assayed by observing larval and pupal movement following stimulation with a pipette tip. The Cox Mixed Effects and Hazard Ratio calculations were performed using R for R 4.0.2 GUI 1.72 for Mac OS at https://www.r-project.org/(R Core Team 2020) and the *coxme* package, version 2.2–16 (Therneau 2020). Oxford reference style it would be: Team RC. R: A language and environment for statistical computing. R Foundation for Statistical Computing, Vienna, Austria. http://wwwR-project.org/ [Internet]. 2022 [cited 2022 Sep 13].

Measurements of phagolysosomal pH

Phagolysosomal pH was measured by an established ratiometric fluorescence technique, as described in previous studies (Fu et al. 2018, Dragotakes et al. 2020). Briefly, BMDM were seeded on glass coverslips in 24-well tissue culture plates at a density of 1.25 × 10^5 cells/well and activated overnight with IFNγ (100 U/ml) and LPS (500 ng/ml). *Cryptococcus neoformans* particles were opsonized with 18B7 monoclonal antibody, which was previously conjugated to Oregon Green 488, at a final concentration of 10 μg/ml and added to the activated macrophages at MOI 1:1. The plates were

centrifuged at 350 × *g* for 1 min to synchronize fungal cell adherence and ingestion by macrophages. After 2 h, media in each well was replaced twice with an equivalent volume of HBSS and the coverslip placed upside down on a MatTek Petri dish with HBSS in the microwell for imaging on an upright scope (Olympus AX70). Ratiometric fluorescence measurements focusing on ingested intracellular *C. neoformans* cells were made using 440 and 488 nm excitation and 520 nm emission. Images were analyzed using Metafluor Fluorescence Ratio Imaging Software to calculate fluorescence ratios. The pH of the phagosome was calculated from interpolation of a standard curve; the standard curve was generated by incubating infected macrophages with HBSS buffer with 10 μM nigericin and of known pH ranging from pH 3 to 7.

Growth assays

The Bioscreen C (Growth Curves USA) was used to evaluate any growth defects in *yor1*Δ strain versus wild-type H99. Cultures were grown Sabouraud rich media overnight from frozen stock. A total of 24 h later, they were counted via hemocytometer before inoculating either Sabouraud or MM at a concentration of 5×10^5 before 10-fold serial diluting to 5×10^2 per ml. A volume of 200 μl of each culture was plated in triplicate on HC-2 honeycomb plates (Growth Curves USA) yielding a starting inoculum of 10^5 down to 10^2 cells per 200 μl well. The plates were run with constant agitation at 37°C for 72 h with a wideband ($OD_{420–580}$) measurement taken every 15 min. Alternatively, growth curves were performed by seeding 10^3 cells/ml in 2 ml media (SAB or MM) in 12-well tissue culture dishes. Cultures were then incubated for 96 h at 30°C with OD600 measurements taken every 2 h on a BioTek Epoch microplate spectrophotometer.

Urease activity assay

A total of three replicate cultures for each strain were inoculated at equivalent densities, 5×10^7 cells/ml, and incubated for 24 h at 30°C in urea broth consisting of 10 mM KH_2PO_4, 0.1% Bacto Peptone (Difco), 0.1% -glucose, 0.5% NaCl, 2% urea, and 0.03 mM phenol red, as described by (PMID 353068). Cell-free supernatants were collected by centrifugation at 10 000 × *g* for 1 min through a Costar Spin-X 0.22 μm filter. Samples of filtrates were transferred to wells of a clear 96-well plate and absorbance at 560 nm was read using a Spectramax M5 MultiMode Microplate reader (Molecular Devices). Following subtraction of background absorbance (measured for a cell-free media control) data were plotted and analyzed for statistical significance using an ordinary one-way analysis of variance (ANOVA) with GraphPad Prism 9 software.

Analysis of EVs

Parental and mutant strains were cultivated in yeast extract–peptone–dextrose (YPD, 5 ml) medium for 24 h (30°C, with shaking). The cell suspensions were adjusted to 3.5×10^7 cells/ml and 300 μl were inoculated onto YPD agar plates ($n = 3$). The cultures were incubated to confluence for 24 h at 30°C.

The cells were gently recovered from each plate with an inoculation loop and suspended in PBS (30 ml). For removal of the cells and debris, the suspensions were first centrifuged at 5000 × *g* for 15 min at 4°C, and the resulting supernatants were centrifuged at 15 000 × *g* for 15 min at 4°C. The supernatants were filtered through 0.45-μm pore syringe filters and centrifuged at 100 000 × *g* for 1 h at 4°C to recover EVs. EVs were analyzed by nanoparticle tracking analysis (NTA) on an LM10 nanoparticle analysis system, coupled with a 488-nm laser and equipped with an SCMOS camera and a syringe pump (Malvern Panalytical, Malvern, United Kingdom), as previously published (Reis et al. 2021). Data were acquired and analyzed using the NTA 3.0 software (Malvern Panalytical).

Bioinformatics analysis

We performed bioinformatics analysis using ExVe (http://exve.icc.fiocruz.br), SignalP (http://www.cbs.dtu.dk/services/SignalP/; Almagro Armenteros et al. 2019), PrediSi (http://www.predisi.de/), and Phobius (https://phobius.sbc.su.se/; Kall et al. 2007). Structure prediction was performed using Phyre2 (http://www.sbg.bio.ic.ac.uk/phyre2/html/page.cgi?id = index; Kelley et al. 2015). Results are displayed in Table S1 (Supporting Information). For Tables in Figure S6 (Supporting Information), RNAseq datasets were downloaded from the indicated publications, through NIH GEO database. Raw data was analyzed by bowtie2 (2.3.5) alignment with the most recent *C. neoformans* H99 and KN99α genome (fungidb.org), count matrices generated with HTSeq (1.99.2), and analyzed with Bioconductor DESeq2 (1.22.2).

Acknowledgments

We acknowledge the help of Dr Emily Chen, from the Herbert Irving Comprehensive Cancer Center (Columbia University Medical Center) proteomics facility.

Supplementary data

Supplementary data are available at *FEMSML* online.

Conflicts of interest. None declared.

Funding

E.H.J., Q.D., L.S.R., D.Q.S., A.D., A.J., C.C., and A.C. were supported by the NIH grants to A.C. (AI052733-16, AI152078-01, and HL059842-19). C.C. was supported by the AMS Springboard Award (SBF006\1024), the Wellcome Trust Institutional Strategic Support Award (WT105618MA) to C.C. via the Translational Research Exchange @ Exeter, and the MRC Centre for Medical Mycology grant (MR/N006364/2) to Gordon D. Brown. This work was supported, in part, by the Intramural Research Program of the National Institutes of Health (AI001123 and AI001124 to P.R.W.).

References

Alanio A, Desnos-Ollivier M, Dromer F, Dynamics of *Cryptococcus neoformans*-macrophage interactions reveal that fungal background influences outcome during cryptococcal meningoencephalitis in humans. *MBio* 2011;**2**:e00158–11. https://doi.org/10.1128/mBio.00158-11.

Almagro Armenteros JJ, Tsirigos KD, Sønderby CK *et al.* SignalP 5.0 improves signal peptide predictions using deep neural networks. *Nat Biotechnol* 2019;**37**:420–3.

Alvarez M, Casadevall A, Phagosome extrusion and host-cell survival after *Cryptococcus neoformans* phagocytosis by macrophages. *Curr Biol* 2006;**16**:2161–5.

Bojarczuk A, Miller KA, Hotham R *et al. Cryptococcus neoformans* intracellular proliferation and capsule size determines early macrophage control of infection. *Sci Rep* 2016;**6**:21489.

Bürgel PH, Marina CL, Saavedra PHV *et al. Cryptococcus neoformans* secretes small molecules that inhibit IL-1β inflammasome-dependent secretion. *Mediat Inflamm* 2020;**2020**:1.

Cangelosi GA, Ankenbauer RG, Nester EW, Sugars induce the agrobacterium virulence genes through a periplasmic binding protein and a transmembrane signal protein. *Proc Natl Acad Sci* 1990;**87**:6708–12.

Casadevall A, Cleare W, Feldmesser M *et al.* Characterization of a murine monoclonal antibody to *Cryptococcus neoformans* polysaccharide that is a candidate for human therapeutic studies. *Antimicrob Agents Chemother* 1998;**42**:1437–46.

Casadevall A, Perfect JR. *Cryptococcus Neoformans*. 1st edn. Washington: Amer Society for Microbiology, 1998.

Chen LC, Blank ES, Casadevall A, Extracellular proteinase activity of *Cryptococcus neoformans*. *Clin Diagn Lab Immunol* 1996;**3**:570–4.

Chen SC, Wright LC, Santangelo RT *et al.* Identification of extracellular phospholipase B, lysophospholipase, and acyltransferase produced by *Cryptococcus neoformans*. *Infect Immun* 1997;**65**: 405–11.

Coelho C, Bocca AL, Casadevall A, The intracellular life of *Cryptococcus neoformans*. *Annu Rev Pathol* 2014;**9**:219–38.

Coelho C, Souza ACO, da Silveira Derengowski L *et al.* Macrophage mitochondrial and stress response to ingestion of *Cryptococcus neoformans*. *J Immunol* 2015;**194**:2345–57.

Core Team R R: A language and environment for statistical computing. *R Foundation for Statistical Computing*. 2020. https://www.R-project.org/

Cox GM, McDade HC, Chen SC *et al.* Extracellular phospholipase activity is a virulence factor for *Cryptococcus neoformans*. *Mol Microbiol* 2001;**39**:166–75.

Cox GM, Mukherjee J, Cole GT *et al.* Urease as a virulence factor in experimental cryptococcosis. *Infect Immun* 2000;**68**:443–8.

Dang EV, Lei S, Radkov A *et al.* Mechanism of innate immune reprogramming by a fungal meningitis pathogen. *Immunology* 2021. doi: 10.1038/s41586-022-05005-4.

Davidson AL, Chen J, ATP-binding cassette transporters in bacteria. *Annu Rev Biochem* 2004;**73**:241–68.

De Leon Rodriguez CM, Rossi DCP, Fu MS *et al.* The outcome of the *Cryptococcus neoformans*-macrophage interaction depends on phagolysosomal membrane integrity. *J Immunol* 2018;**201**:583–603.

De Leon-Rodriguez CM, Fu MS, Çorbali MO *et al.* The capsule of *Cryptococcus neoformans* modulates phagosomal pH through its acid-base properties. *Msphere* 2018;**3**:e00437–18. https://doi.org/10.1128/mSphere.00437-18.

Decottignies A, Grant AM, Nichols JW *et al.* ATPase and multidrug transport activities of the overexpressed yeast ABC protein yor1p. *J Biol Chem* 1998;**273**:12612–22.

DeLeon-Rodriguez CM, Casadevall A, *Cryptococcus neoformans*: tripping on acid in the phagolysosome. *Front Microbiol* 2016;**7**:164.

Djordjevic JT, Role of phospholipases in fungal fitness, pathogenicity, and drug development - lessons from *Cryptococcus neoformans*. *Front Microbiol* 2010;**1**:125.

Dragotakes Q, Fu MS, Casadevall A, Dragotcytosis: elucidation of the mechanism for *Cryptococcus neoformans* macrophage-to-Macrophage transfer. *J Immunol* 2019;**202**:2661–70.

Dragotakes Q, Stouffer KM, Fu MS *et al.* Macrophages use a bet-hedging strategy for antimicrobial activity in phagolysosomal acidification. *J Clin Invest* 2020;**130**:3805–19.

Edman JC, Kwon-Chung KJ, Isolation of the URA5 gene from *Cryptococcus neoformans* var. neoformans and its use as a selective marker for transformation. *Mol Cell Biol* 1990;**10**: 4538–44.

Feldmesser M, Kress Y, Novikoff P *et al. Cryptococcus neoformans* is a facultative intracellular pathogen in murine pulmonary infection. *Infect Immun* 2000;**68**:4225–37.

Fisher JF, Valencia-Rey PA, Davis WB, Pulmonary cryptococcosis in the immunocompetent patient-many questions, some answers. *Open Forum Infect Dis* 2016;**3**:ofw167.

Fu MS, Coelho C, De Leon-Rodriguez CM *et al. Cryptococcus neoformans* urease affects the outcome of intracellular pathogenesis by modulating phagolysosomal pH. *PLoS Pathog* 2018;**14**:e1007144.

Geddes JMH, Croll D, Caza M *et al.* Secretome profiling of *Cryptococcus neoformans* reveals regulation of a subset of virulence-associated proteins and potential biomarkers by protein kinase A. *BMC Microbiol* 2015;**15**:206.

Gerstein AC, Jackson KM, McDonald TR *et al.* Identification of pathogen genomic differences that impact human immune response and disease during *Cryptococcus neoformans* infection. *Mbio* 2019;**10**:e01440–19. https://doi.org/10.1128/mBio.01440-19.

Gilbert AS, Wheeler RT, May RC. Fungal pathogens: survival and replication within macrophages. *Cold Spring Harb Perspect Med* 2014;**5**:a019661.

Hayes JB, Sircy LM, Heusinkveld LE *et al.* Modulation of macrophage inflammatory nuclear factor κB (NF-κB) signaling by intracellular *Cryptococcus neoformans*. *J Biol Chem* 2016;**291**:15614–27.

Henderson DP, Payne SM, *Vibrio cholerae* iron transport systems: roles of heme and siderophore iron transport in virulence and identification of a gene associated with multiple iron transport systems. *Infect Immun* 1994;**62**:5120–5.

Hossain S, Veri AO, Liu Z *et al.* Mitochondrial perturbation reduces susceptibility to xenobiotics through altered efflux in *Candida albicans*. *Genetics* 2021;**219**:iyab095.

Janbon G, Ormerod KL, Paulet D *et al.* Analysis of the genome and transcriptome of *Cryptococcus neoformans* var. grubii reveals complex RNA expression and microevolution leading to virulence attenuation. *PLos Genet* 2014;**10**:e1004261.

Johnston SA, May RC, The human fungal pathogen *Cryptococcus neoformans* escapes macrophages by a phagosome emptying mechanism that is inhibited by arp2/3 complex-mediated actin polymerisation. *PLoS Pathog* 2010;**6**:e1001041.

Jung WH, Saikia S, Hu G *et al.* HapX positively and negatively regulates the transcriptional response to iron deprivation in *Cryptococcus neoformans*. *PLoS Pathog* 2010;**6**:e1001209.

Jung WH, Sham A, White R *et al.* Iron regulation of the major virulence factors in the AIDS-associated pathogen *Cryptococcus neoformans*. *PLoS Biol* 2006;**4**:e410.

Kall L, Krogh A, Sonnhammer ELL, Advantages of combined transmembrane topology and signal peptide prediction–the phobius web server. *Nucleic Acids Res* 2007;**35**:W429–32.

Karpievitch YV, Polpitiya AD, Anderson GA *et al.* Liquid chromatography mass spectrometry-based proteomics: biological and technological aspects. *Ann Appl Stat* 2010;**4**:1797–823.

Kelley LA, Mezulis S, Yates CM *et al.* The phyre2 web portal for protein modeling, prediction and analysis. *Nat Protoc* 2015;**10**:845–58.

Khakhina S, Johnson SS, Manoharlal R *et al.* Control of plasma membrane permeability by ABC transporters. *Eukar Cell* 2015;**14**:442–53.

Kihara A, Igarashi Y, Cross talk between sphingolipids and glycerophospholipids in the establishment of plasma membrane asymmetry. *Mol Biol Cell* 2004;**15**:4949–59.

Kitahara N, Morisaka H, Aoki W *et al.* Description of the interaction between *Candida albicans* and macrophages by mixed and quantitative proteome analysis without isolation. *AMB Expr* 2015;**5**:127. https://doi.org/10.1186/s13568-015-0127-2.

Kumari S, Kumar M, Gaur NA *et al.* Multiple roles of ABC transporters in yeast. *Fung Genet Biol* 2021;**150**:103550.

Li Z, Sun Z, Li D *et al.* Identification of a Zds-like gene ZDS3 as a new mediator of stress resistance, capsule formation and virulence of

the human pathogenic yeast *Cryptococcus neoformans*. *FEMS Yeast Res* 2011;**11**:529–39.

Liu OW, Chun CD, Chow ED *et al.* Systematic genetic analysis of virulence in the human fungal pathogen *Cryptococcus neoformans*. *Cell* 2008;**135**:174–88.

Ma H, Croudace JE, Lammas DA *et al.* Expulsion of live pathogenic yeast by macrophages. *Curr Biol* 2006;**16**:2156–60.

Mansour MK, Reedy JL, Tam JM *et al.* Macrophage cryptococcus interactions: an update. *Curr Fung Infect Rep* 2014;**8**:109–15.

May RC, Stone NRH, Wiesner DL *et al.* Cryptococcus: from environmental saprophyte to global pathogen. *Nat Rev Microbiol* 2016;**14**:106–17.

Missall TA, Pusateri ME, Donlin MJ *et al.* Posttranslational, translational, and transcriptional responses to nitric oxide stress in *Cryptococcus neoformans*: implications for virulence. *Eukar Cell* 2006;**5**:518–29.

Nicola AM, Robertson EJ, Albuquerque P *et al.* Nonlytic exocytosis of *Cryptococcus neoformans* from macrophages occurs in vivo and is influenced by phagosomal pH. *MBio* 2011;**2**:e00167–11. https://doi.org/10.1128/mBio.00167-11.

Nishida S, Tsubaki M, Exploration of molecular targets in the development of new therapeutics aimed at overcoming multidrug resistance. *Yakugaku Zasshi* 2017;**137**:145–9.

Noverr MC, Cox GM, Perfect JR *et al.* Role of PLB1 in pulmonary inflammation and cryptococcal eicosanoid production. *Infect Immun* 2003;**71**:1538–47.

Orsi CF, Colombari B, Ardizzoni A *et al.* The ABC transporter-encoding gene AFR1affects the resistance of *Cryptococcus neoformans* to microglia-mediated antifungal activity by delaying phagosomal maturation. *FEMS Yeast Res* 2009;**9**:301–10.

Parreira V, da SC, Santos LGC *et al.* ExVe: the knowledge base of orthologous proteins identified in fungal extracellular vesicles. *Comput Struct Biotechnol J* 2021;**19**:2286–96.

Perez-Riverol Y, Csordas A, Bai J *et al.* The PRIDE database and related tools and resources in 2019: improving support for quantification data. *Nucleic Acids Res* 2019;**47**:D442–50.

Rajasingham R, Smith RM, Park BJ *et al.* Global burden of disease of HIV-associated cryptococcal meningitis: an updated analysis. *Lancet Infect Dis* 2017;**17**:873–81.

Reboutier D, Piednoël M, Boisnard S *et al.* Combination of different molecular mechanisms leading to fluconazole resistance in a *Candida lusitaniae* clinical isolate. *Diagn Microbiol Infect Dis* 2009;**63**:188–93.

Reis FCG, Gimenez B, Jozefowicz LJ *et al.* Analysis of cryptococcal extracellular vesicles: experimental approaches for studying their diversity among multiple isolates, kinetics of production, methods of separation, and detection in cultures of titan cells. *Microbiol Spectr* 2021;**9**:e0012521. https://doi.org/10.1128/Spectrum.00125-21.

Rizzo J, Wong SSW, Gazi AD *et al.* *Cryptococcus* extracellular vesicles properties and their use as vaccine platforms. *J Extracell Ves* 2021;**10**:e12129. https://doi.org/10.1002/jev2.12129.

Rodrigues ML, Nakayasu ES, Oliveira DL *et al.* Extracellular vesicles produced by *Cryptococcus neoformans* contain protein components associated with virulence. *Eukar Cell* 2008;**7**:58–67.

Schmidt H, Vlaic S, Krüger T *et al.* Proteomics of *Aspergillus fumigatus* Conidia-containing phagolysosomes identifies processes governing immune evasion. *Mol Cell Proteomics* 2018;**17**:1084–96 .

Shao X, Mednick A, Alvarez M *et al.* An innate immune system cell is a major determinant of species-related susceptibility differences to fungal pneumonia. *J Immunol* 2005;**175**:3244–51.

Shekhar-Guturja T, Gunaherath GMKB, Kithsiri Wijeratne EM *et al.* Dual action antifungal small molecule modulates multidrug efflux and TOR signaling. *Nat Chem Biol* 2016;**12**:867–75.

Singh A, Panting RJ, Varma A *et al.* Factors required for activation of urease as a virulence determinant in *Cryptococcus neoformans*. *MBio* 2013;**4**:e00220–13.

Stukes S, Coelho C, Rivera J *et al.* The membrane phospholipid binding protein annexin A2 promotes phagocytosis and nonlytic exocytosis of *Cryptococcus neoformans* and impacts survival in fungal infection. *J Immunol* 2016;**197**:1252–61.

Stukes S, Cohen HW, Casadevall A, Temporal kinetics and quantitative analysis of *Cryptococcus neoformans* non-lytic exocytosis. *Infect Immun* 2014;**82**:2059–67 .

Subramani A, Griggs P, Frantzen N *et al.* Intracellular *Cryptococcus neoformans* disrupts the transcriptome profile of M1- and M2-polarized host macrophages. *PLoS ONE* 2020;**15**:e0233818 .

Sukumaran A, Ball B, Krieger JR *et al.* Cross-kingdom infection of macrophages reveals pathogen- and immune-specific global reprogramming and adaptation. *Mbio* 2022;**13**:e01687–22. https://doi.org/10.1128/mbio.01687-22 .

Sun S, Fu C, Ianiri G *et al.* The pheromone and pheromone receptor mating-type locus is involved in controlling uniparental mitochondrial inheritance in Cryptococcus. *Genetics* 2020;**214**:703–17.

Therneau TM. coxme: mixed effects Cox models. CRAN. 2020.

Tucker SC, Casadevall A, Replication of *Cryptococcus neoformans* in macrophages is accompanied by phagosomal permeabilization and accumulation of vesicles containing polysaccharide in the cytoplasm. *Proc Natl Acad Sci* 2002;**99**:3165–70.

Yu C-H, Chen Y, Desjardins CA *et al.* Landscape of gene expression variation of natural isolates of *Cryptococcus neoformans* in response to biologically relevant stresses. *Microbial Genomics* 2020;**6**:e000319. https://doi.org/10.1099/mgen.0.000319.

Zaragoza O, Alvarez M, Telzak A *et al.* The relative susceptibility of mouse strains to pulmonary *Cryptococcus neoformans* infection is associated with pleiotropic differences in the immune response. *Infect Immun* 2007;**75**:2729–39.

Zhang M, Sun D, Shi M. Dancing cheek to cheek: *Cryptococcus neoformans* and phagocytes. *Springerplus* 2015;**4**:410 .